JOURNAL OF GEOPHYSICAL RESEARCH, VOL. 113, D05301, doi:10.1029/2007JD008678, 2008

QBO and annual cycle variations in tropical lower stratosphere trace gases from HALOE and Aura MLS observations

M. R. Schoeberl,[1] A. R. Douglass,[1] P. A. Newman,[1] L. R. Lait,[2] D. Lary,[2] J. Waters,[3] N. Livesey,[3] L. Froidevaux,[3] A. Lambert,[3] W. Read,[3] M. J. Filipiak,[4] and H. C. Pumphrey[4]

Received 20 March 2007; revised 26 June 2007; accepted 6 December 2007; published 1 March 2008.

[1] We have analyzed thirteen years (1993 to 2005) of HALOE and over two years of EOS MLS observations (September 2004 to December 2006) for QBO and annual cycle trace variations in tropical H_2O, HCl, ozone, N_2O, CO, HF, and CH_4. We use these results to develop the theory explaining both Brewer-Dobson circulation (BDC) and QBO driven fluctuations in tropical trace gases. For H_2O, BDC variations drive part of the tropopause annual forcing through annual variations in the temperature as has been shown previously. For CO, the annual variations in the BDC amplify the annual fluctuations in CO at the tropopause as has recently been shown by Randel et al (2007). In both cases, the tropopause signal is carried upward by the mean BDC. For ozone, N_2O, HCl and other gases, photochemical processes force fluctuations in the trace gases to be synchronized with annual and QBO variations in the zonal mean residual vertical velocity as is shown using lag correlations.

Citation: Schoeberl, M. R., et al. (2008), QBO and annual cycle variations in tropical lower stratosphere trace gases from HALOE and Aura MLS observations, *J. Geophys. Res.*, *113*, D05301, doi:10.1029/2007JD008678.

1. Introduction

[2] Annual cycle variations exhibited by lower stratospheric water vapor (i.e., the tape recorder) are a result of tropical isolation, the mean Brewer-Dobson circulation (BDC) upwelling and tropopause variations in temperature during the annual cycle [*Mote et al.*, 1996, 1998]. The isolation and upwelling of the tropical lower stratosphere are also evident in higher tropical mixing ratios of N_2O and CH_4, and lower tropical amounts of inorganic chlorine, compared to extratropical latitudes. Measurements of SF_6 and CO_2 show that tropical lower stratospheric air is significantly younger than extra-tropical air [*Waugh and Hall*, 2002], which also indicates the isolation of that region.

[3] In the water vapor tape recorder, seasonal changes in tropical tropopause water vapor mixing ratio rise nearly unperturbed through the lower stratosphere to from 20–30 km. Any trace gas that has seasonal variations in its mixing ratio at the tropical tropopause and has a lifetime greater than months in the lower stratosphere should produce a tape recorder signal as the variations are carried upward by the tropical upwelling. For example, CO, which seasonally varies at the tropical tropopause due to biomass burning, also produces a tape recorder signal [*Schoeberl et al.*, 2006]. A tape recorder signal is also evident in HCN, which is occasionally enhanced by biomass burning [H. Pumphrey, personal communication, 2006] and CO_2 [*Andrews et al.*, 1999]. The tropical upwelling of the BDC is driven by the dissipation of extratropical planetary waves in the mid-stratosphere through the downward control principal [*Haynes et al.*, 1991] and may vary in magnitude during the season and from year to year.

[4] The dynamical isolation of the tropics also makes the tropical quasi-biennial oscillation (QBO) possible [e.g., *Dunkerton*, 1991]. The QBO consists of alternate East-West direction stratospheric winds descending from about 30 km to the tropopause with a period of about 26–27 months [see review by *Baldwin et al.*, 2001]. The QBO is confined to the tropics although the oscillation induces secondary circulations in the extratropics and affects the extra-tropical latitudes through changes in planetary wave ducting. A description of the QBO, its tropical and extratropical effects, and the theory of the QBO are reviewed by Baldwin et al. op. cit. The secondary circulation associated with the QBO is superimposed upon the BDC. The QBO secondary circulation consists of an increase in the upwelling during the easterly shear phase and a suppression of the upwelling during the westerly phase [*Plumb and Bell*, 1982]. At the peak of the easterly circulation, the QBO secondary circulation is divergent with air flowing away from the equator. This flow reverses at the peak of the westerly circulation.

[5] The QBO and Brewer-Dobson circulations modified the constituent distributions in the tropical stratosphere. The QBO, for instance, is clearly evident in tropical ozonesonde data [*Logan et al.*, 2003 and references therein] as well as satellite aerosol data [*Trepte and Hitchman*, 1992; *Grant et al.*, 1996] and satellite trace gas data [*Hasebe*, 1994;

[1] NASA Goddard Space Flight Center, Greenbelt, Maryland, USA.
[2] University of Maryland Baltimore County, Baltimore, Maryland, USA.
[3] NASA Jet Propulsion Laboratory, Pasadena, California, USA.
[4] School of GeoSciences, The University of Edinburgh, Edinburgh, UK.

0148-0227/08/2007JD008678$09.00

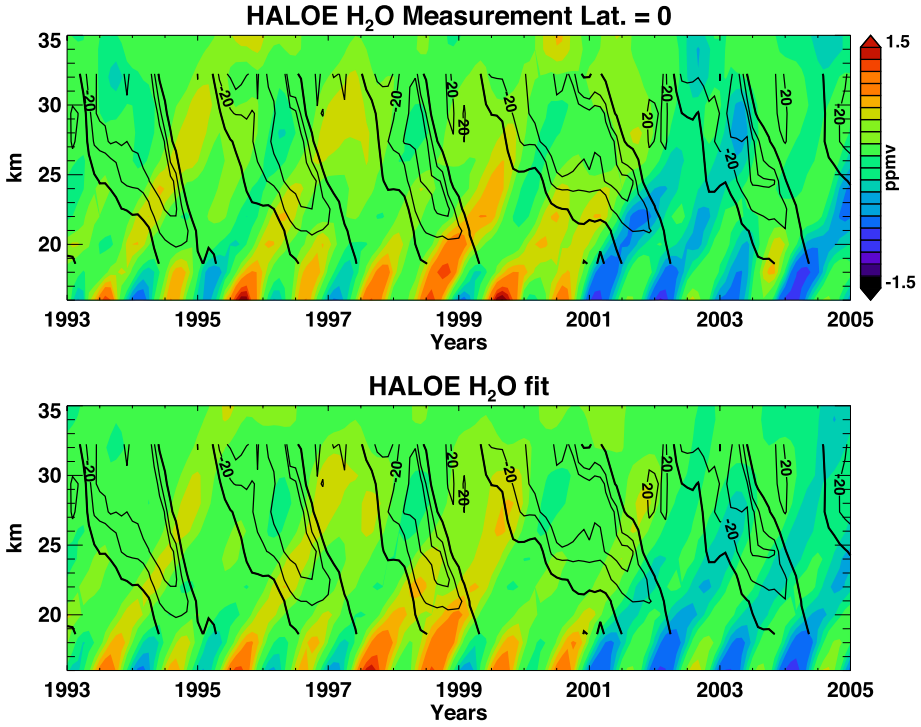

Figure 1. The equatorial water vapor anomalies from HALOE data (top). Water vapor field from the SVD fit (bottom). Singapore winds (m/s) are over-plotted on the figure.

Hollandsworth et al., 1995; *Randel and Wu*, 1996; *Schoeberl et al.*, 1997; *Randel et al.*, 1998].

[6] A good portion of the Halogen Occultation Experiment (HALOE) trace gas data record has been analyzed for trace gas fluctuations by *Dunkerton* [2001] (hereafter D2001). D2001 used rotated principal component analysis to extract QBO, semi-annual, annual and subbiennial components for ozone, CH_4, and H_2O. The subbiennial components are evidently due to non-linear interactions between the annual cycle and the QBO. D2001 showed that the subtropical anomalies were larger in the Northern Hemisphere, and he was also able to reproduce the trace gas variations using standard harmonics combined with a decadal variation. D2001 was also able to identify the seasonal synchronization of the annual cycle with the QBO in the trace gas data.

[7] In this paper we analyze 11 years of tropical HALOE trace gas distributions from 1994–2005) of observations from the aboard the UARS satellite and two years of Earth Observing System Microwave Limb Sounder (MLS) data aboard the Aura satellite. We extend the analysis of D2001 to include HCl and HF, and add CO and N_2O from MLS.

[8] The MLS and HALOE instruments make measurements in quite different ways: HALOE is an infrared solar occultation instrument and MLS is a microwave limb sounder. MLS makes measurements about every 1.5° in latitude with fourteen passes across the equator each day. HALOE made tropical measurements only a few times a month. Between the two instruments, O_3, H_2O and HCl were common measurements. HALOE also measured CH_4 and HF as well as nitrogen radicals and aerosols. MLS also measures N_2O, CO and other trace gases.

[9] Our goal is to quantify and explain the annual and QBO variations in the satellite trace gas measurements. We are extending the D2001 analysis over a longer record using a single value decomposition analysis employing standard harmonics.

2. Analysis of the Trace Gas Data

[10] First, zonal monthly mean v19 HALOE [*Russell et al.*, 1993] and v1.5 MLS [*Waters et al.*, 2006] data sets are constructed. In the case of HALOE, the data are binned into 5° latitude zones; 2° latitude zones are used for MLS. Where occasional missing data occurs in the monthly mean time series, temporal linear interpolation from earlier and subsequent data is used to fill the gap. We avoid the pre-1993 HALOE data because of retrieval problems associated with the dense Pinatubo stratospheric aerosols. The MLS data sequence is from September 2004–December 2006, barely encompassing a single QBO cycle.

[11] To perform the analysis, the data is reformed into a time series for each latitude and altitude grid point. A least squares fit is performed to a linear trend combined with annual, semi-annual, and QBO harmonics. Following D2001 and *Randel and Wu* [1996], the data are least squares fit to a set of functions that includes a linear trend and annual, semi-annual and QBO harmonics. Singular value decomposition (SVD) is used derive coefficients. This approach allows us to explain nearly all the variance in the tropical trace gas data. Although the QBO can vary in frequency, we assume a fixed frequency of 25.2 months for HALOE and 28 months for MLS (due to the shorter data record). The period is determined from a Fourier transform power spectral analysis of the QBO wind field over the period. For the HALOE data set, the discrete Fourier transform periods near the standard QBO period of 26–

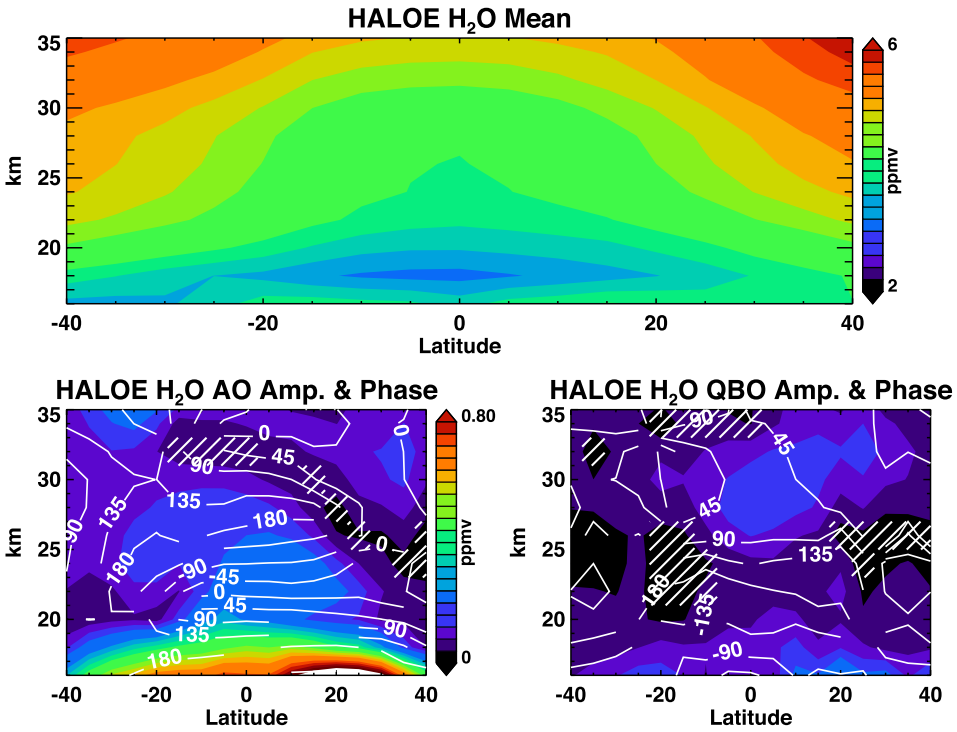

Figure 2. Top, zonal mean, time mean water vapor from 13 years of HALOE data. Bottom left, amplitude and phase of the annual oscillation (AnO). Bottom right, amplitude and phase of the QBO oscillation. Phase measured from the beginning of the analysis period, January 1993 so decreasing phase with altitude indicate upward propagating signals. Cross hatching indicates regions where the 95% confidence limit is not met.

27 months are 30, 25.2 and 21 months. Nearly all the spectral power shows up in the 25.2 month period.

[12] The components of the SVD fit are checked for statistical significance. As each new function (annual, QBO, etc.) was added to the fit, an *F* test was used to determine whether the new fit was a statistically significant improvement over the previous fit in terms of reducing the residual variance [see, for example, *Mandel*, 1964]. Using the null hypothesis that the new fit made no difference, and assuming that the grid points are mutually independent, the 95% significance level was used in determining the threshold value for the *F* statistic above which the null hypothesis was rejected. Although the grid points are not actually independent of each other, the results may be taken as a rough indication of where the signals are likely to be meaningful.

[13] Because of the short time record of the MLS data, some of the biennial inter-annual variation will show up as a QBO signal. This is most evident at midlatitudes so we will concentrate most of our discussion on the annual and QBO signal in the tropics.

2.1. Annual and QBO Cycles in the HALOE and MLS Constituent Data

[14] Trace gas variations in the stratosphere between the tropopause and ~35 km fall into two types: those strongly synchronized with the zonal mean circulation at the altitude of the fluctuation (whether that zonal mean circulation is driven by the BDC or by the QBO) and those whose fluctuations can be traced back to BDC changes at the tropopause. Ozone, for example, falls into the first category and H_2O, the second. CO appears to be a mixed type.

[15] We begin our analysis by examining the trace gas fluctuations themselves. In the section below, we restrict our analysis to the trace gases H_2O, O_3, HCl and CO. The first three are common to both HALOE and MLS. Other tracers, HF and CH_4 for HALOE, and N_2O for MLS are discussed in Appendix A.

[16] In our analysis, we report the amplitude and phase of the annual oscillation (AnO) and the QBO. The phases are reported relative to the beginning of the analysis. For HALOE this is January 1993; for MLS this is September 2004.

2.2. Water Vapor

[17] Figure 1 shows the HALOE water vapor anomalies (top) data and the SVD fit reconstruction (bottom). Upward-progressing annual variations in water vapor are clearly evident. This is the water vapor "tape recorder." The tape recorder signal was first identified in UARS MLS and HALOE water vapor data by *Mote et al.* [1996]. Also evident in the figure is the decrease in water vapor in the later years [*Randel et al.*, 2006]. The fit shown in the bottom panel of the figure reasonably captures the interannual and long-term variability of water vapor. Simulation of the secular decrease in tropical water vapor required additional long-term components to the SVD fit in addition to the linear trend in order to reduce the variance.

[18] Figure 2 shows the mean HALOE H_2O field along with the annual and QBO component amplitudes and

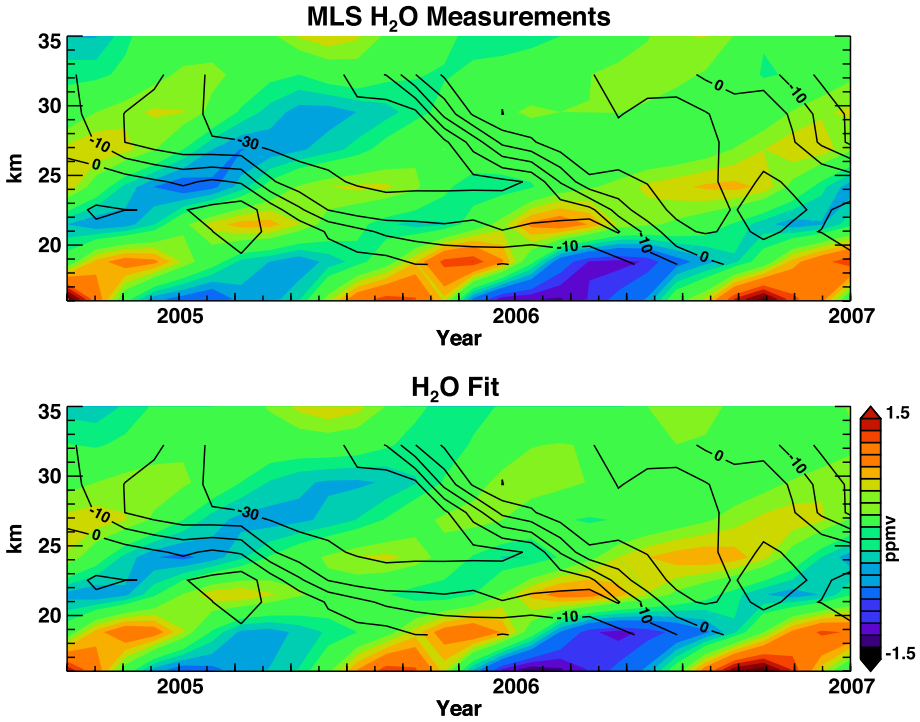

Figure 3. Equatorial EOS MLS water vapor anomalies as in Figure 1.

phases. The mean field shows a drier zone near the top of the tropical tropopause that extends southward and downward as noted by *Rosenlof et al.* [1997]. The annual oscillation (AnO) shows the coherent regular phase variation with altitude characteristic of the tape recorder. In this convention, the upward propagating signal will show a phase decrease with altitude.

[19] At low altitudes, the amplitude of the annual signal is stronger north of the equator, which is not surprising since the wet phase of the tape recorder is strongly forced by the

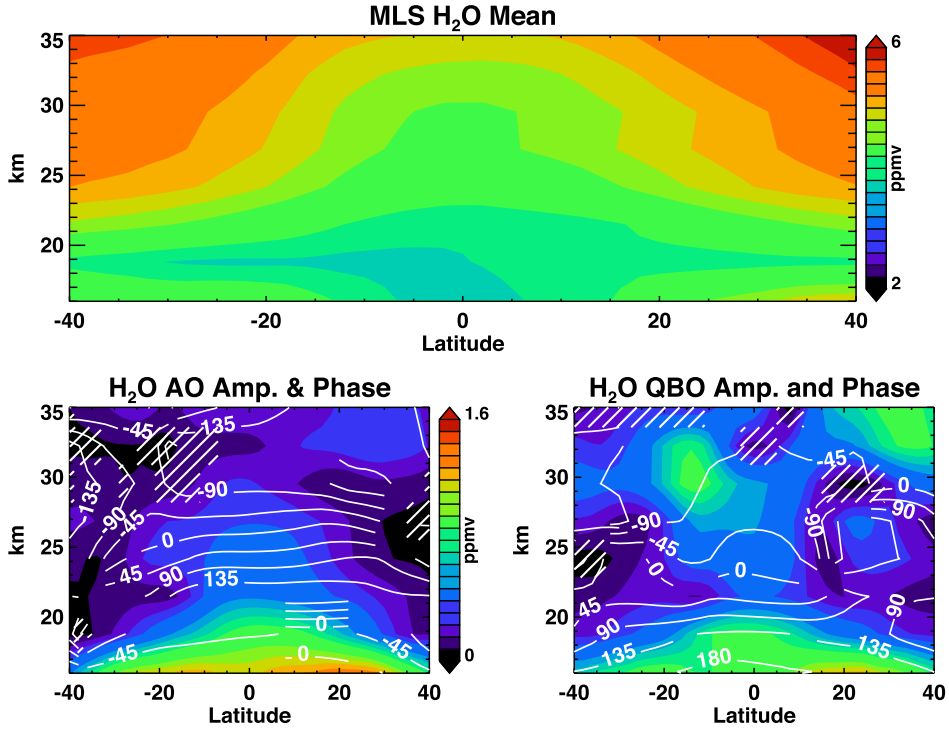

Figure 4. Same as Figure 2 for MLS H_2O.

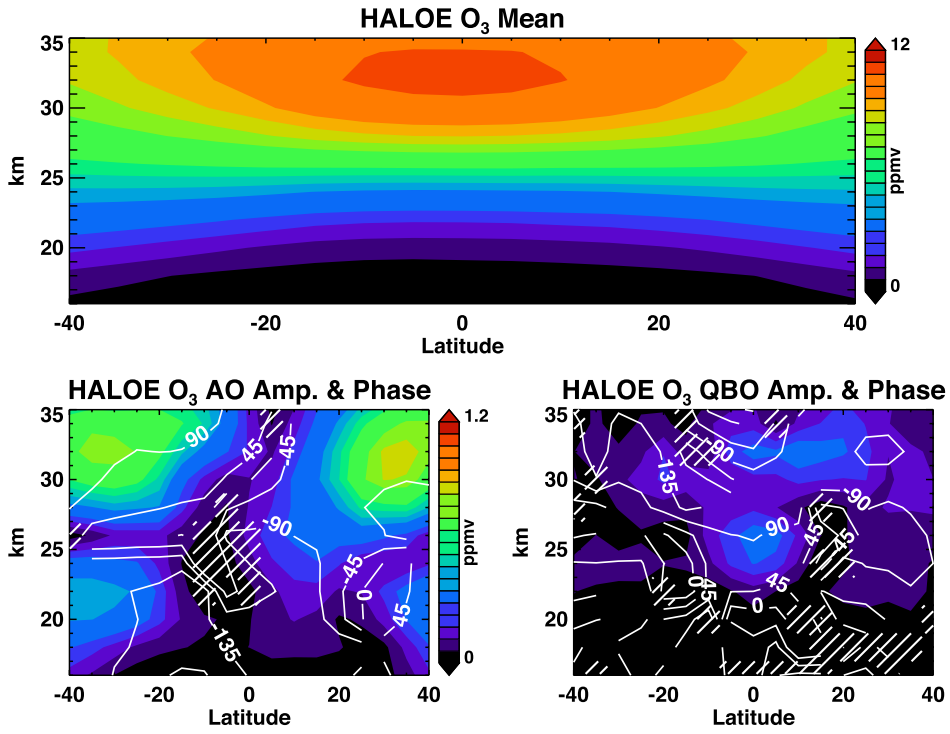

Figure 5. Same as Figure 2 for HALOE O_3. except lower figure s show changes in % rather than mixing ratio.

Himalayan monsoon [*Dunkerton*, 1995; *Randel et al.*, 2001; *Gettelman et al.*, 2004]. Figure 2 also shows that there is a weak QBO water vapor signal mostly at upper levels. The QBO signal is also evident in Figure 1 where a modulation in the tape recorder occurs when the QBO shear zones descend across the water vapor anomalies in 2000 and 2003 near 20 km. As found by D2001, the amplitude of the signal is higher in the Northern Hemisphere. Note that the phase also decreases with altitude although the QBO descends. As will be shown below, the phase of tracers anomalies is also determined by the mean gradient of the anomaly field.

[20] Figure 3 shows the water vapor anomalies from EOS MLS for the period September 2004–December 2006. As with the HALOE data, the fitting procedure does a good job reproducing the data. Figure 4 shows the results for the analysis of 28 months of MLS observations. The mean field is generally similar although MLS water vapor mixing ratios are slightly higher; preliminary validation shows that MLS water vapor is about 10–15% higher than HALOE [*Froidevaux et al.*, 2006]. We also note that the low tropical MLS water vapor field is significantly narrower in latitude than the HALOE field. By selecting shorter periods of HALOE data analysis, we can reproduce the narrower field in the MLS data (not shown). Thus it is the 13 years of interannual variation in the location of the tropical stratospheric dry zone that produces the wider tropical average in HALOE.

[21] The MLS annual amplitude and phase (Figure 4) are similar to HALOE results (Figure 2) including a slight shift in amplitude toward the Northern Hemisphere (NH) in the lower stratosphere and a bend in the amplitude toward the south near 26 km. The QBO amplitude and phase are also similar, although the magnitude is larger consistent with a sharper vertical and horizontal gradient in the MLS H_2O mixing ratio.

2.3. Ozone

[22] The ozone QBO has been previously identified in the column measurements [*Bowman*, 1989; *Hollandsworth et al.*, 1995; *Randel and Wu*, 1996] and in profile measurements from Stratospheric Aerosol and Gas Experiment II (SAGE II) data [*Zawodny and McCormick*,1991; *Hasebe*, 1994; *Randel and Wu*, 1996], HALOE data (D2001) and ozonesonde data [*Logan et al.*, 2003].

[23] Figure 5 shows our results for HALOE ozone, we now also show the percent amplitude relative the mean value to bring out the structure in the UTLS. The QBO signal peaks near 24–26 km as noted by D2001 and is remarkably symmetric about the equator. This symmetry can be explained as follows: the QBO secondary circulation vertical motion field has its peak amplitude at the equator, and this vertical motion field acting on the mean gradient produces the structure in Figure 5 bottom right. The lack of a meridional gradient in the mean ozone field suppresses any contribution by off-equatorial QBO that result from QBO meridional secondary circulation.

[24] The tropical annual oscillation in ozone is only statistically significant below 20 km and above 30 km and the amplitude is quite high relative to the mean in the lower tropical stratosphere (see percentage plot, Figure 5 lower left). As noted by *Randel et al.* [2007], the annual oscillation in lower stratospheric ozone is due to the annual variation of the BDC acting on the mean ozone vertical gradient. Outside of the tropics near 30 km, the annual oscillation is strong and is probably driven by annual variations in the residual circulation (the meridional and

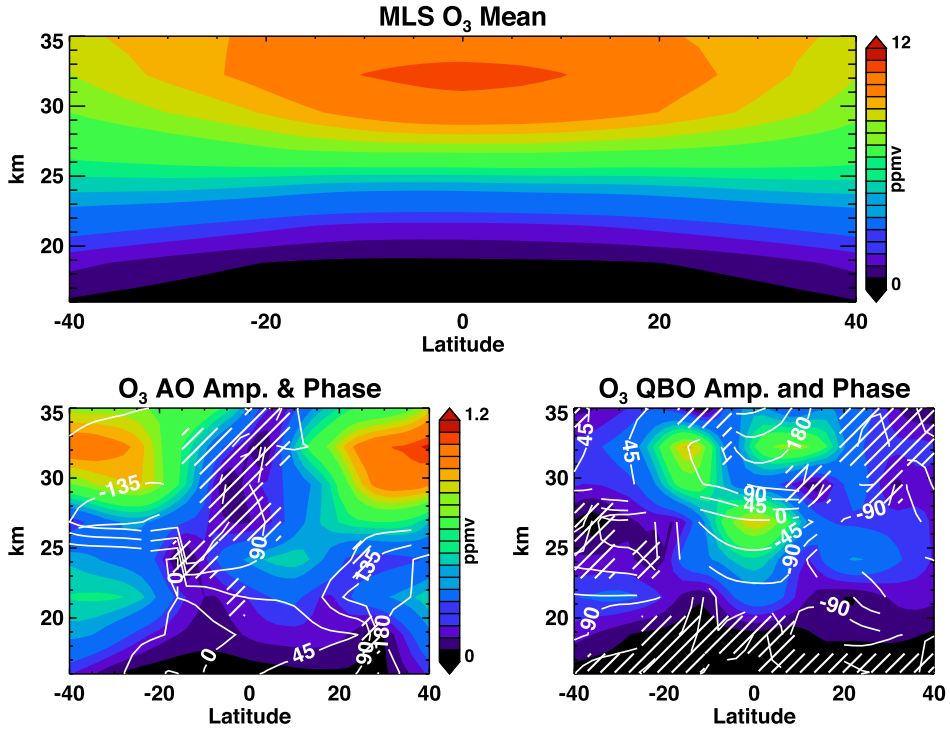

Figure 6. Same as Figure 5 except for MLS O_3.

vertical advective components of the BDC) as indicated by weak phase shift between the tropical lower stratosphere region and the northern midlatitude region.

[25] Figure 6 shows the analysis for MLS ozone which should be compared to Figure 5. The picture from MLS generally confirms the picture from HALOE, but there are several differences worth noting. The peak in the MLS QBO signal is stronger and is near 27 km, about two km higher than HALOE. We also see clear secondary peaks in the QBO in the subtropics above 30 km where the meridional ozone gradient is larger (see D2001).

[26] In the MLS AnO field a signature from 5°N near 24 km connects to a stronger feature at 30 km and 30°N also seen in the HALOE data. Again, the lack of phase difference with the tropopause region suggests that this AnO feature is connected to the extratropical BDC. The increase in AnO amplitude with altitude at the equator is consistent with the increase in the ozone vertical gradient with increasing altitude. Both HALOE and MLS show (in the percentage plots) strong annual amplitude structure in the tropical upper troposphere peaking at about 8–12°N, roughly the mean position of the ITCZ.

2.4. HCl

[27] HCl forms from the reaction of Cl with CH_4 following photolysis of chlorine-containing halogens (e.g., chlorofluorocarbons) rising in the tropical stratosphere. Surface observations of the dominant long-lived chlorine species show very weak annual variations (e.g., WMO, 2007). Because production of HCl increases slowly with height, HCl has a weak vertical gradient and will have very small annual variations at the tropical tropopause.

[28] Figure 7 shows our analysis of the HALOE HCl data. The AnO signal is very weak but detectable in the lower tropical stratosphere where the HCl mixing ratio is low. The tropical stratospheric AnO signal can only form because of annual variations in the vertical velocity in the lower stratosphere. This kind of variation will not produce a phase shift with altitude, in contrast to the water vapor case.

[29] Stronger extratropical AnO signals exist where the meridional gradient in HCl is large and these signals presumably arise due to the effect of the BDC acting on the horizontal gradient. The low HCl zonal mean tropical upward bulge moves from side to side with the seasonal cycle. This would produce the two peaks in the AnO amplitude, one on either side of the equator.

[30] The QBO signal in HCl has a peak at the equator just above 30 km with an extension into the NH and a smaller secondary peak in the SH. The off-equator signals may be due to the meridional circulation associated with the QBO acting on the time mean meridional gradient of HCl or it may be the effect of the QBO on midlatitude planetary wave breaking and meridional mixing of HCl.

[31] Figure 8 shows the MLS HCl results. MLS HCl is 10–15% higher than HALOE HCl [*Froidevaux et al.*, 2006] on average. In addition to this offset, MLS HCl shows a narrower tropical bulge compared to HALOE (also see Figures 2 and 4 for H_2O). This means the meridional gradients in HCl are larger and the subsequent AnO and QBO signals driven by meridional advection and mixing will be larger. The best example of this effect is the peak in the HCl QBO signal near 20°N at 25 km that is clearly seen in the MLS data (Figure 8) but is nearly absent in the HALOE data (Figure 7). Looking at the mean fields in both figures, there a sharp meridional gradient in HCl in the MLS data at this altitude and latitude that, in the HALOE data, is much weaker. A similar feature is seen in the

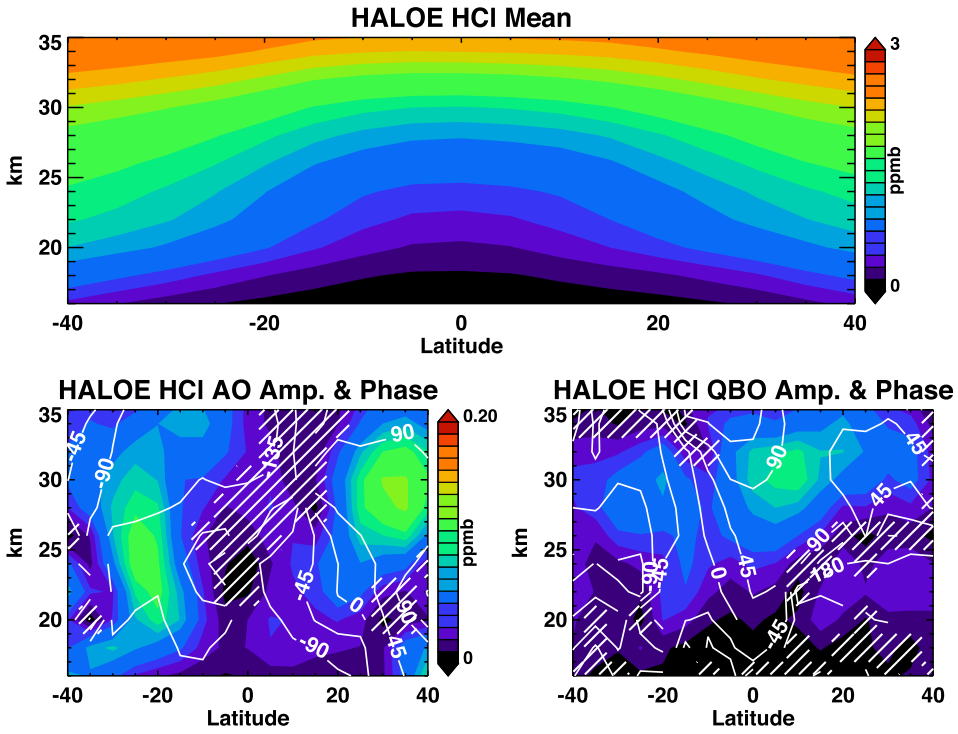

Figure 7. Same as Figure 5 for HALOE HCl.

Southern hemisphere near 30 km and 20°S. In general, however, most of the features seen in the HALOE HCL have corresponding features in the MLS HCL.

2.5. MLS CO

[32] CO has a chemical lifetime of only a few months in the stratosphere due to reaction with OH [*Schoeberl et al.*, 2006]. The tropospheric source is primarily biomass and fossil fuel burning. Figure 9 shows the analysis of MLS CO. MLS CO has a positive bias in the lower stratosphere compared to other CO measurements [*Froidevaux, L. et al.*, 2006]. Because of the weak horizontal and vertical gradients above 20 km, the tropical QBO signal is not

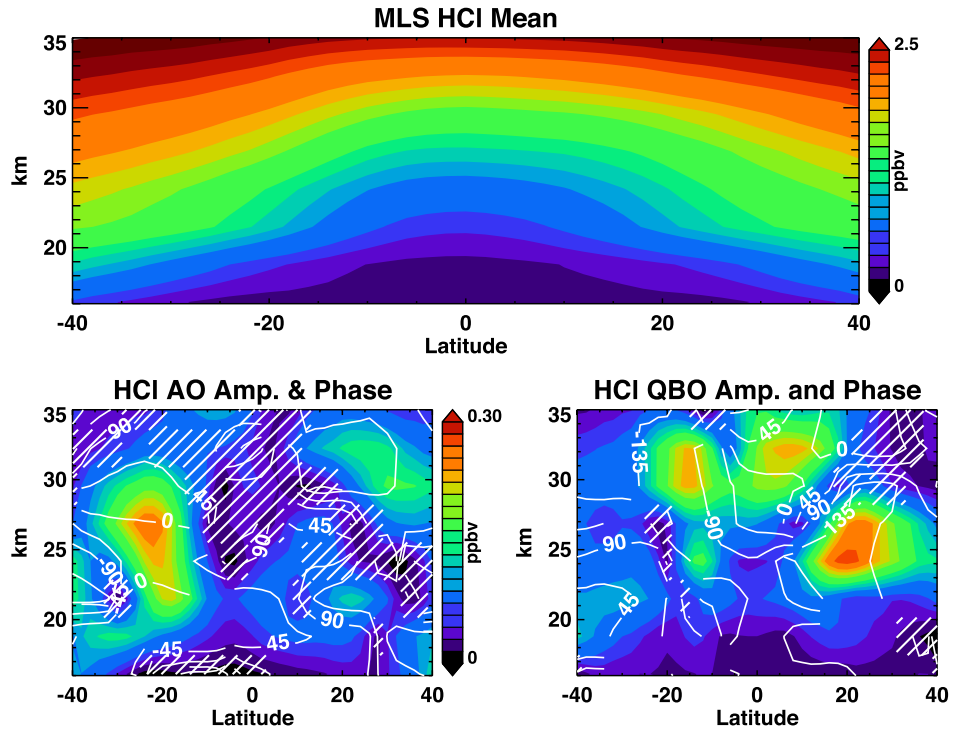

Figure 8. Same as Figure 7 for MLS HCl.

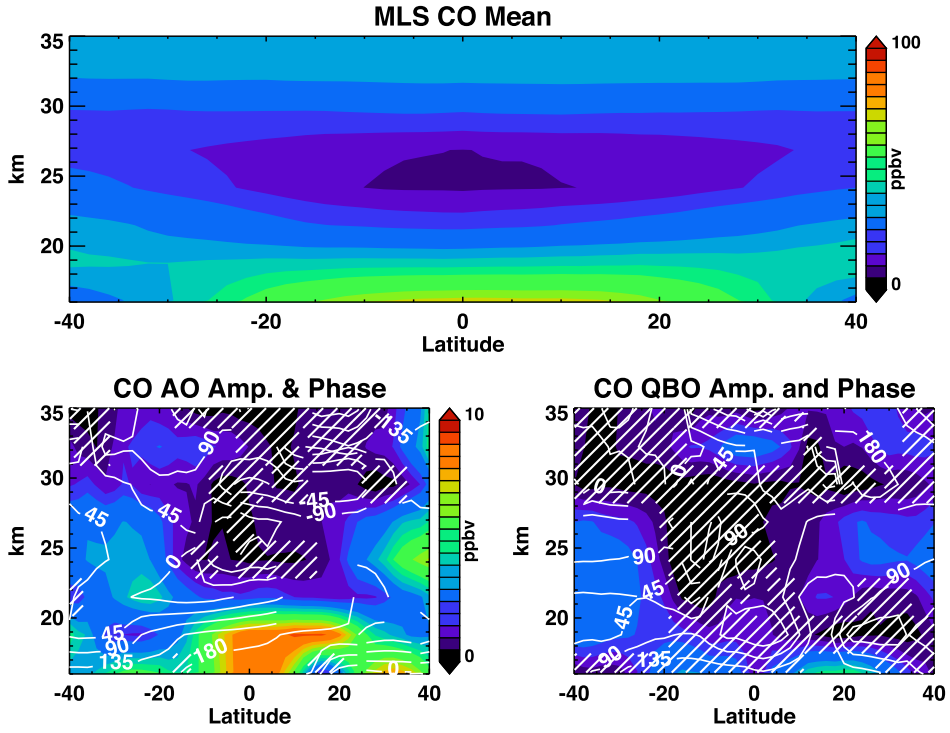

Figure 9. Same as Figure 4 for MLS CO.

present. More interesting is the annual cycle. The increase in amplitude of the AnO between 18 and 20 km is due to the annual variation in the strength of the Brewer-Dobson circulation acting on the strong vertical gradient in CO in the UTLS [*Randel et al.*, 2007]. However, the tape recorder signal is still evident as the regular phase shift in the CO AnO with altitude between 18 and 22 km [*Schoeberl et al.*, 2006].

[33] Comparing Figure 6 with Figure 9 we note that the ozone and CO signals at 18 km are ~180° out of phase. *Folkins et al.* [2006] argued that the anti-correlation of UTLS CO and ozone was due to convection. In their model, convection brings up high CO amounts and low boundary layer ozone so the two are anti-correlated. *Randel et al.* [2007] pointed out that annual variation in the strength of the BDC produces the same effect because the vertical gradients in ozone and CO are opposite. They were able to reproduce the observed variations using the residual vertical velocity acting on the mean gradient. The existence of the AnO maximum in CO between 18 and 20 km argues for the *Randel et al.* [2007] mechanism. The *Folkins et al.* [2006] mechanism should produce a CO peak at lower altitudes than is seen and an amplitude that decreases with height following decreasing convective detrainment with altitude.

3. The Dynamics of Tape Recorder and the QBO Trace Gas Perturbations

[34] In this section we lay out the dynamical mechanisms behind the variations in trace gases due to the QBO and Brewer Dobson circulation. If μ is the volume mixing ratio of a trace gas then to first order [*Mote et al.*, 1998],

$$\frac{\partial \overline{\mu}}{\partial t} + \overline{w}^* \frac{\partial \overline{\mu}}{\partial z} + \overline{v}^* \frac{\partial \overline{\mu}}{\partial y} = \overline{S} - \overline{L} + K \frac{\partial^2 \overline{\mu}}{\partial y^2} \tag{1}$$

where K parameterizes the meridional eddy mixing from the extratropics and $\overline{v}^*$ and $\overline{w}^*$ are the zonal residual meridional and vertical velocities, respectively. The overbar represents zonal mean, t is time, z is the log-pressure height, y is the meridional distance, S is the chemical source and L is the chemical loss rate. The vertical residual velocity is approximated as $\overline{w}^* = \overline{Q}/\overline{\Theta}_z$, where $\overline{Q}$ is the isentropic diabatic heating rate and $\overline{\Theta}_z$ is the potential temperature vertical gradient. We neglect vertical diffusion by breaking gravity waves as this is not very important in the lower stratosphere.

[35] Now we consider a periodic trace gas variation driven by advection and source terms and linearize around the QBO or AnO frequency neglecting the eddy mixing from the tropics to midlatitudes which is small [*Mote et al.*, 1998]

$$\begin{aligned} i\sigma_j \overline{\mu}_j &+ \overline{w}_j^* \frac{\partial \langle \overline{\mu} \rangle}{\partial z} + \langle \overline{w}^* \rangle \frac{\partial \overline{\mu}_j}{\partial z} + \overline{v}_j^* \frac{\partial \langle \overline{\mu} \rangle}{\partial y} + \langle \overline{v}^* \rangle \frac{\partial \overline{\mu}_j}{\partial y} \\ &= \overline{S}_j - \alpha \overline{\mu}_j + K_j \frac{\partial^2 \langle \overline{\mu} \rangle}{\partial y^2} + \langle K \rangle \frac{\partial^2 \overline{\mu}_j}{\partial y^2} \end{aligned} \tag{2}$$

where the subscript j indicates a periodic variation such as the QBO (Q) or AnO (A). The j subscripted variables are ~exp($i\sigma_j t$) and the other variables with $\langle\ \rangle$ are time

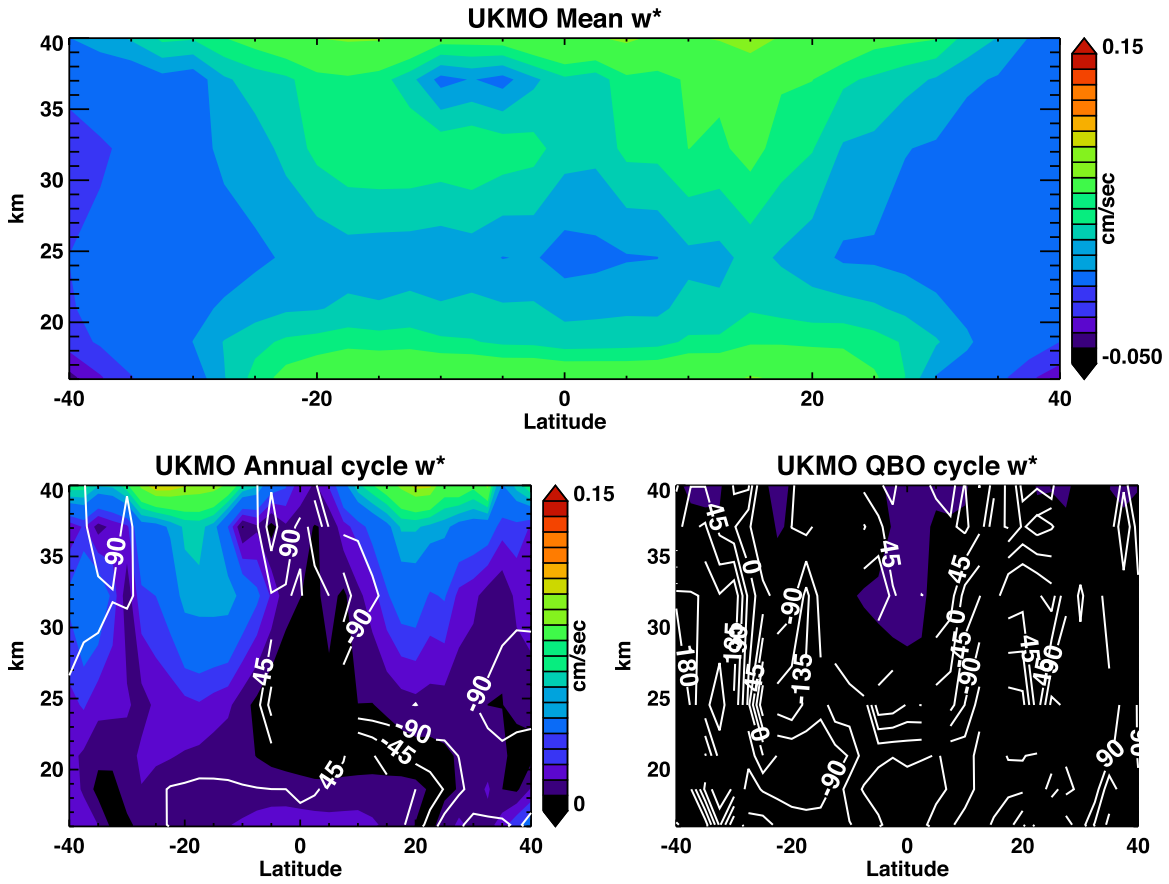

Figure 10. Residual circulation, w^*, from UKMO analysis. Upper figure, time mean component, lower left, annual oscillation, lower right, QBO component. White lines show phase.

averaged. We have assumed that chemical production and loss can be linearized around a mean state. Chemical loss rate perturbations relax to the mean state with a time constant $1/\alpha$ where α is the chemical loss rate, σ is the frequency.

[36] In the simplest AnO case, we assume that the sources and sinks are zero, the mean vertical gradients and all the meridional gradients are zero. In this case, the 1st and 3rd terms on the LHS of (2) are in balance. If $\langle \overline{w}^* \rangle$ is constant with altitude, the dispersion equation is $\lambda_z = 2\pi \langle \overline{w}^* \rangle / \sigma_A$ where λ_z is the vertical wavelength and is σ_A is the frequency. This is the tape recorder case and the mixing ratio $\mu_A = \mu_T \exp(i\sigma_A t + i2\pi z/\lambda_z)$ is determined by the tropopause forcing (μ_T). The phase ($2\pi z/\lambda_z$) changes with altitude as is seen in the tape recorder. *Mote et al.* [1998] included the extra-tropical mixing term in (2) ($\langle K \rangle \frac{\partial^2 \overline{\mu}_j}{\partial y^2}$) and used the amplitude of the tape recorder signal to diagnose K. Consistent with earlier studies of the QBO [e.g., *Schoeberl et al.*, 1997] they found that K was very small in the lower stratosphere. At 22 km the mixing timescale was 80 months. Above 26 km, however, the mixing timescale was estimated to be less than 20 months. We note that the effect of time mean mixing can be incorporated into α, that is $\alpha = \alpha_{\text{chemistry}} + \langle K \rangle L^{-2}$ where L is the meridional length scale of the tropical perturbation. We neglect the annual and QBO variations in K(K_j) which are likely smaller than $\langle$K$\rangle$.

[37] In the case discussed by *Randel et al.* [2007] the annual variation of the Brewer-Dobson circulation drives the annual fluctuations in ozone and CO near the tropopause. For that situation $\left(\overline{w}_A^* \frac{\partial \langle \overline{\mu} \rangle}{\partial z}\right) \gg \left(\langle \overline{w}^* \rangle \frac{\partial \overline{\mu}_A}{\partial z}\right)$, so the LHS 1st and 2nd terms of (2) are dominant. K is assumed zero. Thus $\overline{\mu}_A = i\frac{\overline{w}_A^*}{\sigma_A} \frac{\partial \langle \overline{\mu} \rangle}{\partial z}$ which is equivalent to equation (4) in Randel op cit. Note that the phase variation with altitude is dictated by $\overline{w}_A^*$, and that the mixing ratio response will be 90° degrees out of phase with $\overline{w}_A^*$. This solution suggests there will be no apparent upward phase propagation as seen with the tape recorder.

[38] These two extreme cases explain the two different kinds of equatorial phase variation with altitude associated with the AnO seen in H_2O, CO, O_3 and HCl above as well as N_2O, HF shown in the Appendix. In the case of O_3, N_2O, HF and HCl we see almost no AnO phase shift with altitude in the very lowest part of the tropical stratosphere. These annual variations are thus driven by the BDC's annual variations. In the case of H_2O, a strong phase propagation signal with altitude shows that the AnO in the tropopause forcing is providing a signal that is simply carried upward. CO is a mixed case with no phase shift below ~18–20 km and a phase shift above suggesting a strong Brewer-Dobson component of the annual cycle below 18–20 km with a standard tape-recorder signal above. In the case of CO, it is the very rapid reduction of the vertical gradient with altitude that allows CO to shift behavior from BDC forcing to a tape recorder signal.

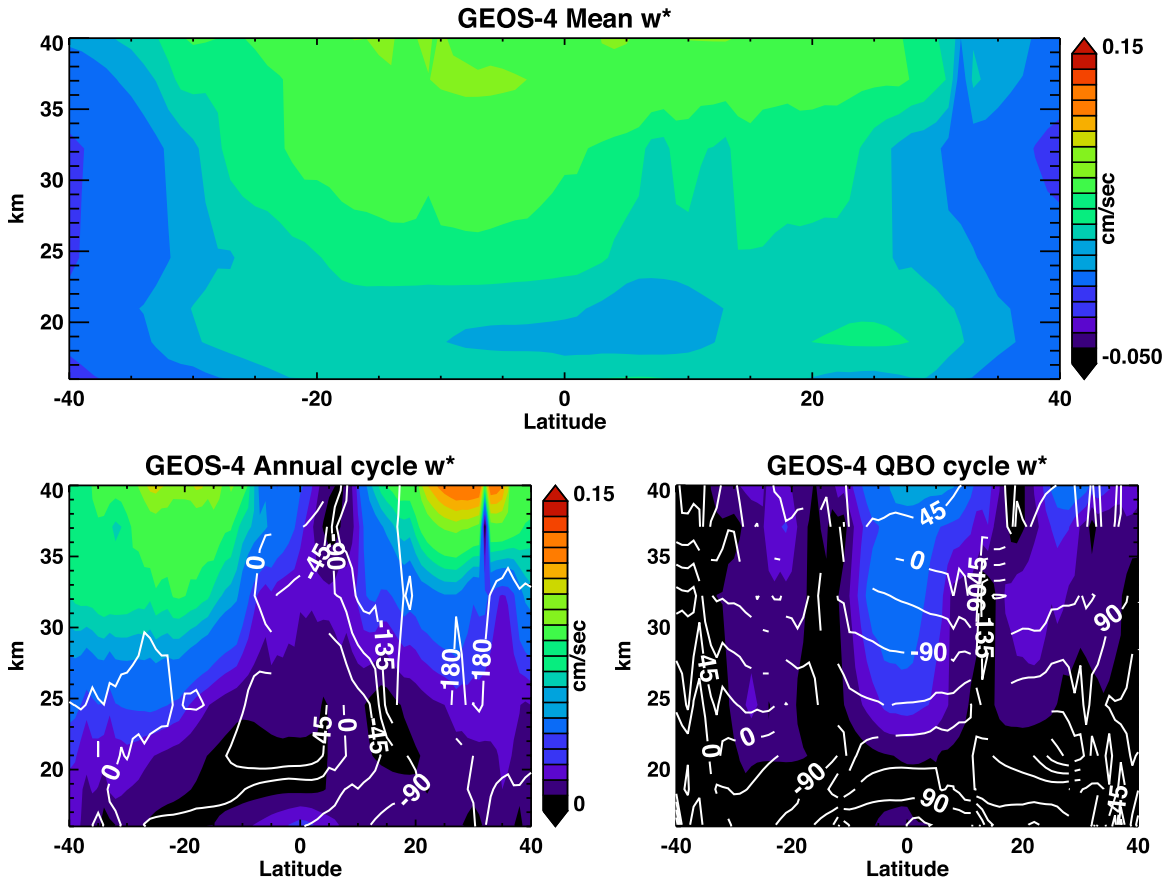

Figure 11. Same as Figure 10 except for GEOS-4 assimilation White lines show phase.

[39] An alternative approach to showing the Brewer-Dobson and advective effects is to reform the equations as a Lagrangian transport system. Equation (2) can be rewritten as

$$\frac{d\overline{\mu}_A}{dt} = S_A - \alpha\overline{\mu}_A - \left(\overline{w}^*_A \frac{\partial\langle\overline{\mu}\rangle}{\partial z} + \overline{v}^*_A \frac{\partial\langle\overline{\mu}\rangle}{\partial y}\right) \qquad (3)$$

where the total derivative $d\overline{\mu}_A/dt$ is the Lagrangian residual tendency, it has the mean advection terms (3rd and 5th in equation (2)) folded together with the partial time derivative. The Brewer-Dobson forcing can now be seen as a kind of "chemical source/sink" term.

[40] Parcels move upward since $\overline{w}^* > 0$. In the case of CO, CO decreases with altitude so the 3rd term on the RHS of (3) term will increase $\overline{\mu}_A$ as seen between 16 and 18 km in Figure 9. For the case of water vapor near the tropopause, (3) shows how changes in the mean temperature processes can affect the tape recorder signal since $\overline{w}^*_A \sim T_A$ through the diabatic heating term and $S_A \sim T_A$ through the Clausius-Clapeyron equation.

4. Mean, Annual and QBO Transport Fields

[41] Using diabatic heating rates and assimilated temperatures, we can compute $\overline{w}^*$. The heating rate is adjusted so that the global integral of $\overline{w}^*$ is zero at each pressure level for mass continuity. For the HALOE period we use the United Kingdom Meteorological Office (UKMO) meteorological fields [*Swinbank and O'Niell*, 1994; *Randel et al.*, 2004]. Heating rates for these fields are computed off-line as described by *Rosenfield et al.* [1994]. For the MLS period we use GEOS-4 assimilated meteorological fields [*Bloom et al.*, 2005]. The $\overline{w}^*$ mean, annual cycles, and QBO amplitudes and phases for 1993–2005 (UKMO) and 2003–2006 (GEOS-4) are calculated using the same SVD analysis. The results are shown in Figures 10 and 11, respectively.

[42] *Randel et al.* [2004] have analyzed the stratospheric climatologies of several assimilation systems. Among other things, they looked at the mean tropical biases and model representation of the stratospheric QBO and semi-annual oscillations. The UKMO (called METO in their study) mean tropical 100 hPa temperatures are systematically ~2 K warmer than ERA-40 temperatures (ERA-40 is comparable to GEOS-4). This would put ERA-40 further from radiative equilibrium and increase the tropopause diabatic heating, which would increase $\overline{w}^*$ in ERA-40 compared to UKMO. In other words, a colder tropopause will cause increased diabatic heating and increased diabatic uplift. This is consistent with the differences in the mean fields shown in Figures 10 and 11.

[43] Comparison of the UKMO and ERA-40 assimilation QBO wind fields by *Randel et al.* [2004] show that UKMO zonal winds are roughly 20–30% weaker than the observed Singapore winds. The ERA-40 winds show almost no bias compared to observations below 30 km. From the equatorial thermal wind equation, the wind bias between the two assimilation systems should propagate into the estimate of

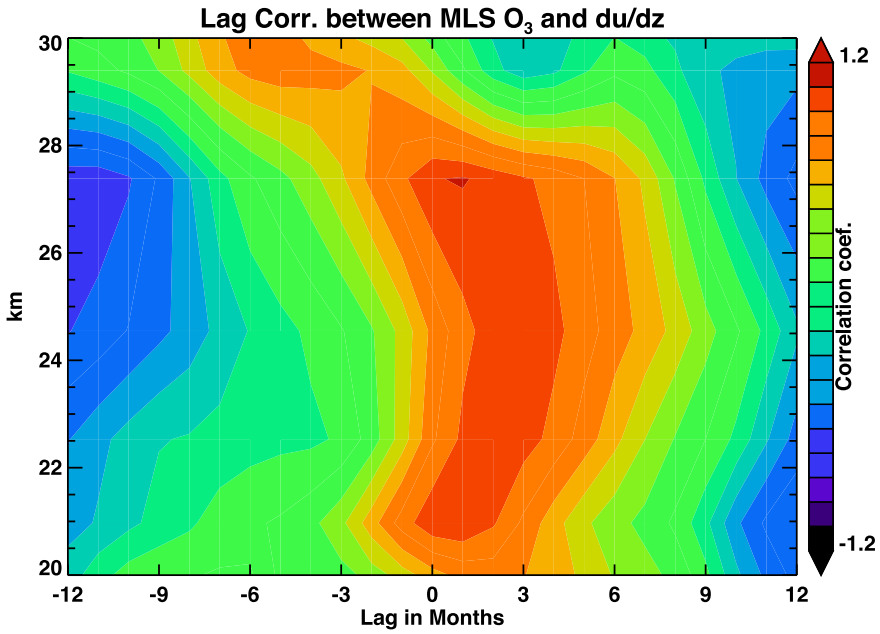

Figure 12. Lag correlation between the vertical wind shear and the ozone perturbation field.

the QBO thermal field and the residual circulation. The differences between the assimilation systems would explain some of the differences in QBO $\overline{w}^*$ fields shown in Figures 10 and 11.

[44] The time mean $\langle \overline{w}^* \rangle$ field is the driver for the tape recorder signal. Figures 10 and 11 show broad regions of upwelling from roughly 30°N to 30°S. The upwelling decreases with altitude near 25 km in the UKMO analysis and 18–20 km in the GEOS-4 analysis. These analyses suggest that there should be a widening of the tape recorder phase above 20 km as the BDC weakens. Such widening is evident in Figure 2 near 24 km.

[45] Figures 10 and 11 also show that the tropical annual cycle in the residual circulation is strongest near the tropopause, decreasing with altitude. The QBO residual circulation is strongest in the GEOS 4 analysis and the tropical phase structure is clearly visible in Figure 11. Note that the QBO phase increases with altitude indicating a descending oscillation.

5. Linkage Between the Mean Fields and the Trace Gas Oscillations

[46] A simple way to link the changes in trace gases with the circulation is to plot the correlation between the trace gas perturbation field lagged with the residual circulation.

[47] It is straightforward to show using the thermal wind equation that T_{QBO} is correlated with the vertical wind shear [see *Andrews et al.*, 1987; *Baldwin et al.*, 2001]. Since the diabatic heating rate will be anticorrelated with T_{QBO}, it follows from (2) that

$$\overline{\mu}_{QBO} \sim \frac{\partial \overline{u}_{QBO}}{\partial z} \frac{\partial \langle \overline{\mu} \rangle}{\partial z} / \left(\alpha + i \left(\sigma_{QBO} + \langle w^* \rangle \gamma \right) \right) \qquad (4)$$

where γ is the vertical wave number of the QBO perturbation. Since the chemical time constant for ozone (α) in the lower stratosphere is faster than the other terms in the denominator (~1 month at these altitudes, *Brasseur and Solomon*, 1986), the ozone perturbations should be highly correlated with the QBO vertical wind shear. This is seen in Figure 12. We also expect that the correlation coefficient would be slightly out of phase from exact synchronization with the wind shear due to the inertial terms in the denominator of (4) and that the correlation would begin to reverse when ozone mean vertical gradient begins to weaken (Figure 6) as is also seen in Figure 12.

[48] In the above example, correlation of the trace gas with the zonal wind shear is essentially a filter that passes the QBO component of $\overline{w}^*$; however, using the $\overline{w}^*$ analysis fields themselves (Figures 10 and 11) we can look at the correlations in general. Figure 13 shows three correlations, HALOE O_3, H_2O, HCl.

[49] Figure 13a shows that ozone is strongly anticorrelated with UKMO $\overline{w}^*$ with almost no phase lag. Because ozone increases with altitude, upward motion fluctuations will produce lower ozone amounts hence the strong anticorrelation. It is important to remember that $\overline{w}^*$ includes the velocity perturbations associated with seasonal BDC and the QBO. Because of the rapid chemical relaxation time ozone, the perturbations generated by the vertical motion field and ozone tend to stay in synchronization, in other words to first order $\overline{\mu}_j \sim -\overline{w}_j^* \frac{\partial \langle \overline{\mu} \rangle}{\partial z} / \alpha_j$. The slight phase lag is due to the inertial terms included in (4) that become more important at lower altitudes where the ozone time constant becomes longer than a month. (Note that in Figure 12, the ozone shows a phase lead because $w^*_{QBO} \sim -\frac{\partial \overline{u}_{QBO}}{\partial z}$.) Ozone shows secondary correlation peaks at ±6 months at 16 km moving to ±12 months peaks near 25 km. The lowest correlation peak is due to annual cycle synchronization; ozone fluctuations anticorrelated with the annual cycle will be correlated with that same cycle 6 months later. Higher up we are seeing the correlation with the QBO cycle; ozone is anticorrelated with the QBO $\overline{w}^*$ field but will become correlated a cycle later, ~12 months.

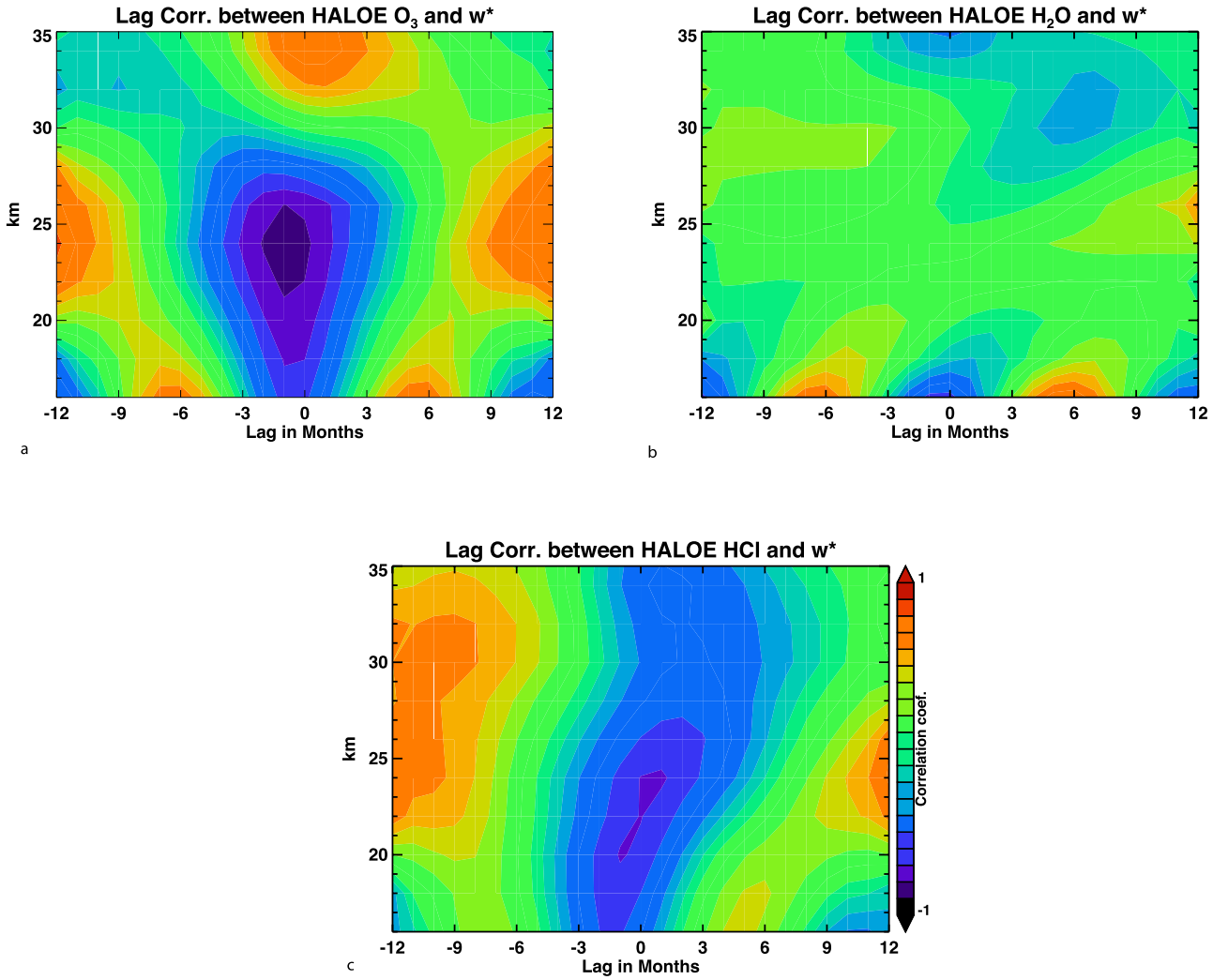

Figure 13. Part a, lag correlation of equatorial HALOE ozone with UKMO w^*, part b with H_2O and part c with HCl.

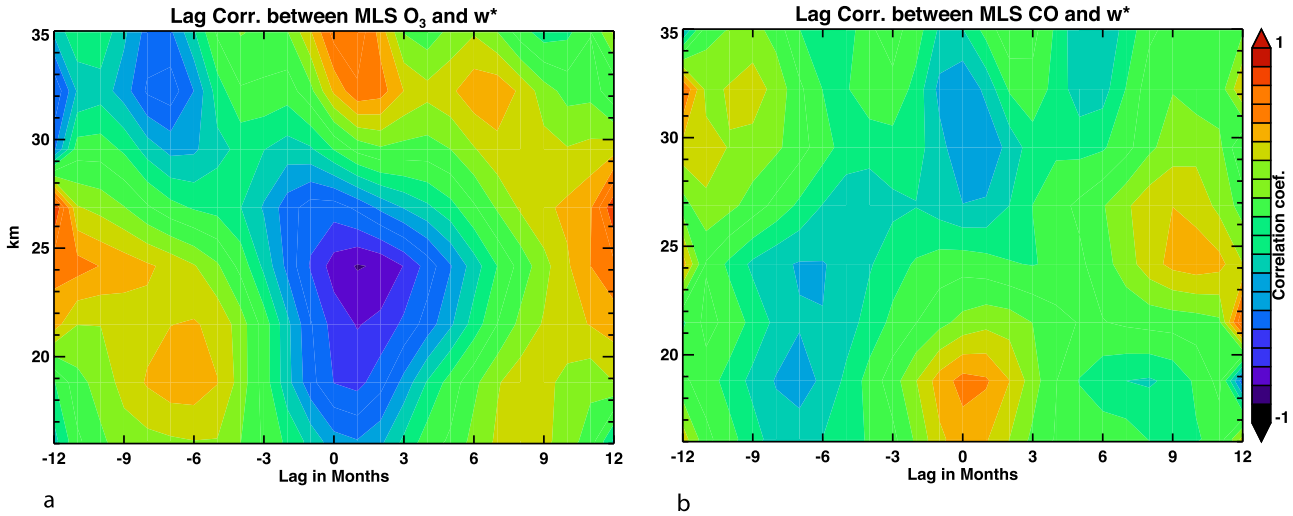

Figure 14. Part a, lag correlation of equatorial MLS ozone with GEOS-4 w^*, part b with CO.

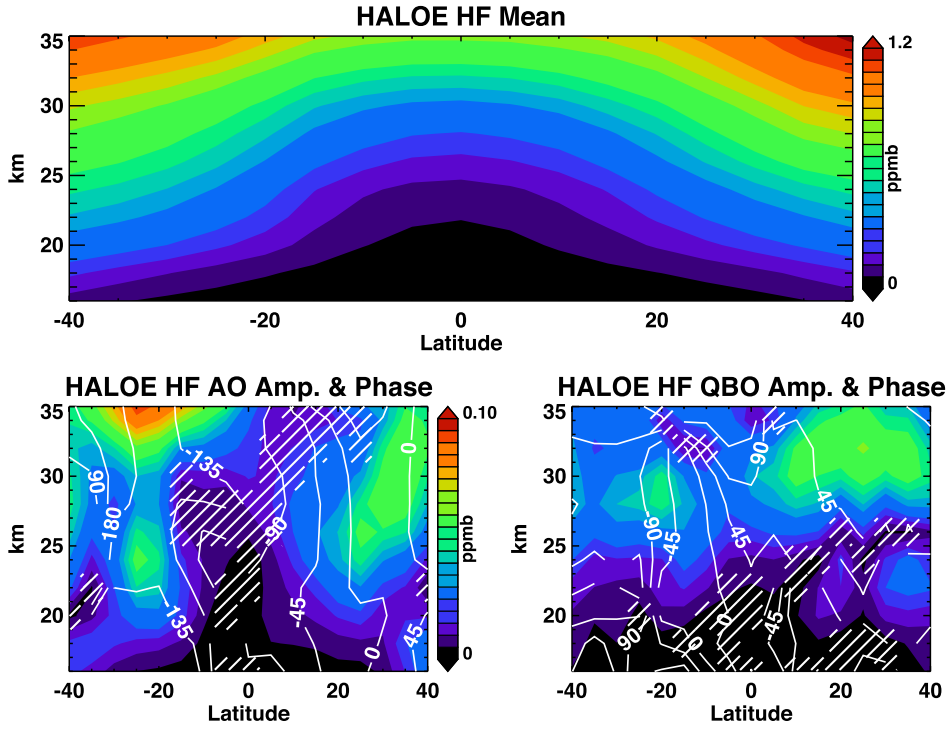

Figure A1. Same as Figure 2 except for HALOE HF.

[50] The correlation plot for water is quite different (Figure 13b). The synchronization with $\overline{w}^*$ is strong only near the tropopause where water vapor fluctuations are controlled by the BDC annual variations. The figure shows that the correlation shifts with altitude as expected with the tape recorder signal. The case of HCl shown in Figure 13c is similar to that of ozone; we see a shift from annual control near the tropopause, due to the mean vertical gradient in HCl, to QBO control at 25 km.

[51] Figure 14 shows the correlation plots for MLS and the $\overline{w}^*$ field from GEOS-4. The ozone correlation (Figure 14a) is very similar to that produced from the HALOE analysis (Figure 13a), providing a check on that analysis. Figure 14b shows the analysis for CO. As discussed above, the figure

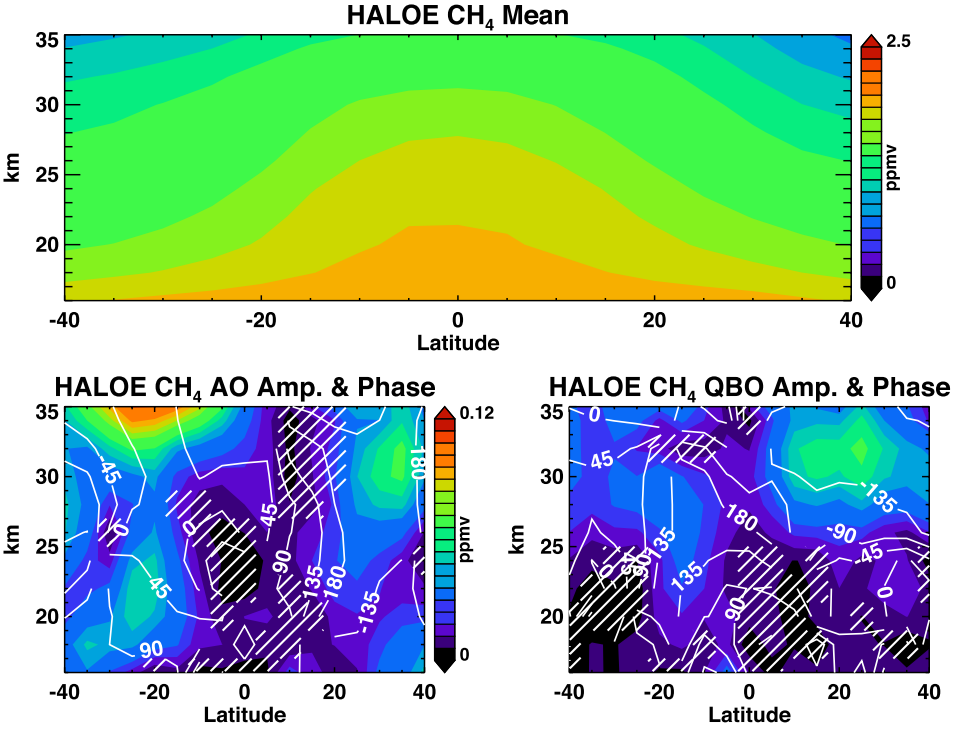

Figure A2. Same as Figure 2 for HALOE CH_4.

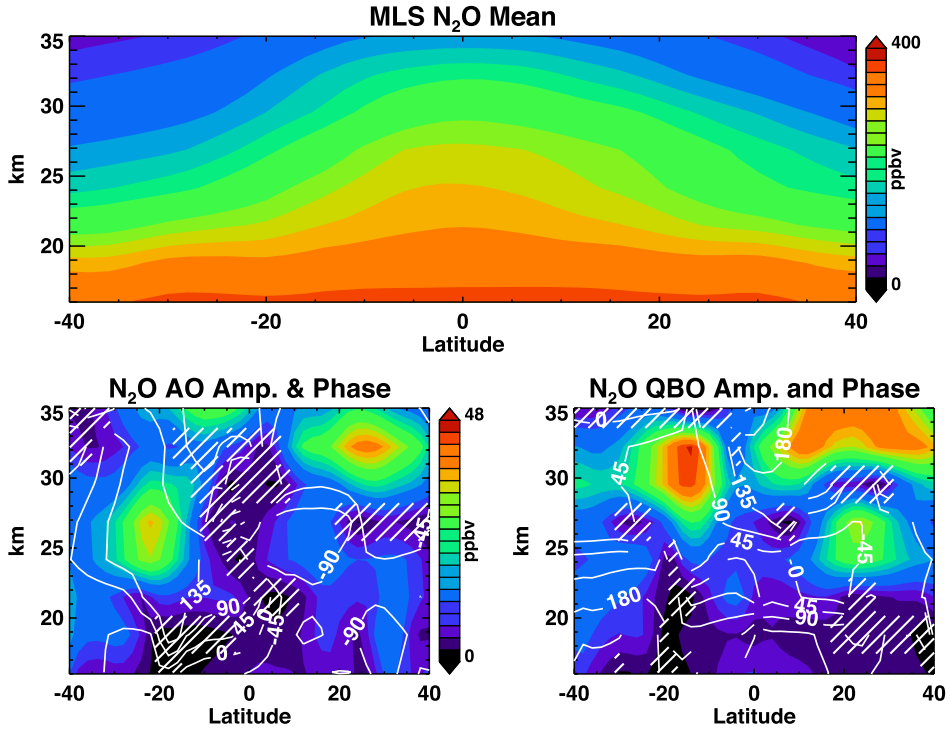

Figure A3. Same as Figure 2 for MLS N_2O.

shows that CO is strongly synchronized with the annual variation in the BDC below 20 km (note the maximum with zero phase lag and two minimum near ±6 months). The correlation shifts above 20 km and a phase slight lag is evident; this is the CO tape recorder [*Schoeberl et al.*, 2006]. Above 26 km CO becomes anticorrelated with $\overline{w}^*$ which is expected since the vertical gradient reverses at 25 km as seem in Figure 9.

[52] To make a more quantitative analysis of the lag correlations we would need to use a full chemical transport model because the chemical time constants are only estimated here. Such an analysis would no doubt give more insight into model behavior compared to observations.

6. Summary

[53] We have analyzed thirteen years of HALOE O_3, H_2O, HF, HCl and CH_4 measurements and 30 months of EOS MLS O_3, H_2O, HCl, CO and N_2O measurements for QBO and AnO signals using a joint SVD fit to those cycles. Our HALOE analysis is similar to that performed by D2001 over a shorter data record.

[54] Trace gas data from both instruments show AnO and QBO signals. These signals are broadly consistent between the instruments although there are small structural and magnitude differences in the mean, annual and QBO fields. These differences can probably be attributed to the differences in the sensors and the different lengths of the time series.

[55] Using the equations of motion we note that when the chemistry is weak and there is an annual variation in the tracer field at the tropopause, then a "tape recorder" signal will emerge. A tape recorder signal is characterized by progressive phase variation with altitude driven by the time mean $\overline{w}^*$ field. The tape recorder signal is mostly independent of the annual variations or QBO variations in the vertical motion fields because they are weaker than the time mean BDC – although the upward phase progression may be perturbed by those variations. If the chemical time constants are more rapid then the tracer variations tends to be phase locked to the circulation (BDC + QBO). We demonstrate this phase locking using lag correlation plots between tracer fluctuations and $\partial\overline{u}/\partial z$ (which isolates the QBO secondary circulation) and lag correlations between the tracer and the $\overline{w}^*$ field that includes both QBO circulation and the annual BDC variations.

Appendix A

A1. Annual and QBO Cycles in the HALOE Unique Constituent Data

A1.1. HALOE HF

[56] Like HCl, HF mainly originates from the photolysis of CFC-11, 12, 113, HCFC-22, Halons 1211 and 1301 and increases in altitude in the stratosphere.

[57] Figure A1 shows the results for HF. These HF results show similar features to the HALOE HCl (see Figure 7). As with HCl two peaks in the QBO signal are seen at 30 km straddling the equator, and two extra tropical peaks in the AnO signal are also seen. In the percentage plots, we also see the tropical annual oscillation peak just north of the equator that is also visible in the HCl measurements.

A1.2. HALOE CH_4

[58] Figure A2 shows the HALOE methane signal that was also analyzed by D2001. Methane rises from the tropical troposphere into the stratosphere where it reacts with OH, Cl, and $O(^1D)$. Methane thus has the opposite meridional gradient from HCl and HF, so we expect to see the same pattern in amplitude for QBO and AnO features as HCl but with opposite phase. Figure A2 shows that this is indeed the

case – both NH and SH features visible in HF and HCl are reproduced in CH_4 with the phase shifted by ~180°.

A1.3. MLS N_2O

[59] Nitrous oxide, like methane, rises through the tropical troposphere and is destroyed by a reaction with $O(^1D)$ or photolysis. As with HALOE CH_4, we expect that the features shown will be quite similar to HCl, except the phase of the AnO and QBO will be 180° off.

[60] Figure A3 displays the N_2O signal (compare to MLS HCl, Figure 8). As expected from the discussion above, the overall features shown in Figure 8 are reproduced in Figure A3 with slightly different amplitudes and nearly 180° phase shift. The differences in the amplitudes can be attributed to the differences in the mean gradient between HCl and N_2O. At these altitudes and latitudes photochemistry is not significant, with one exception. Note the increase in amplitude in the HCl AnO in Figure 8 at the southern edge of the plot. Even though N_2O shows a weak feature near that region, the HCl feature is stronger. The likely explanation is the influence of the chemistry of the ozone hole on HCl. HCl is drawn down during the formation of the ozone hole and then rapidly increases afterward [*Douglass et al.*, 1995; *Santee et al.*, 2005], which would increase the AnO signal.

[61] **Acknowledgments.** The first author acknowledges helpful discussions with W. Randel on the causes of CO variations at the tropopause. The work was supported by NASA Earth Sciences Program.

References

Andrews, D. G., J. R. Holton, and C. B. Leovy (1987), *Middle Atmosphere Dynamics*, 489 pp., Academic, San Diego, Calif.

Andrews, A. E., et al. (1999), Empirical age spectra for the lower tropical stratosphere from in situ observations of CO_2: Implications for stratospheric transport, *J. Geophys. Res.*, *104*(D21), 26,581–26,595.

Baldwin, M. P., et al. (2001), The quasi-biennial oscillation, *Rev. Geophys.*, *39*, 179–229.

Bloom, S., et al. (2005), Documentation and validation of the Goddard Earth Observing System (GEOS) Data Assimilation System-Version 4, *Technical Report Series on Global Modeling and Data Assimilation 104606*.

Bowman, K. P. (1989), Global patterns of the quasi-biennial oscillation in total ozone, *J. Atmos. Sci.*, *46*, 3328–3343.

Brasseur, G., and S. Solomon (1986), *Aeronomy of the Middle Atmosphere*, 452 pp., D. Reidel, Boston, Ma.

Douglass, A. R., et al. (1995), Interhemispheric differences in springtime production of HCl and Clono2 in the polar vortices, *J. Geophys. Res.*, *100*, 13,967–13,978.

Dunkerton, T. J. (1991), Nonlinear propagation of zonal winds in an atmosphere with Newtonian cooling and equatorial wavedriving, *J. Atmos. Sci*, *48*, 236–263.

Dunkerton, T. J. (1995), Evidence of meridional motion in the summer lower stratosphere adjacent to monsoon regions, *J. Geophys. Res.*, *100*, 16,675–16,688.

Dunkerton, T. J. (2001), Quasi-biennial and subbiennial variations of stratospheric trace constituents derived from HALOE observations, *J. Atmos. Sci.*, *58*, 7–25.

Folkins, I., P. Bernath, C. Boone, A. M. Thompson, K. Walker, and J. C. Witte (2006), Seasonal cycles of O3, CO and convective outflow at the tropical tropopause, *Geophys. Res. Lett.*, *33*, L16802, doi:10.1029/2006GL026602.

Froidevaux, L., et al. (2006), Early validation analyses of atmospheric profiles from EOS MLS on the Aura satellite, *IEEE TGRAS*, *44*, 1106–1121.

Gettelman, A., D. E. Kinnison, T. J. Dunkerton, and G. P. Brasseur (2004), The impact of monsoon circulations on the upper troposphere and lower stratosphere, *J. Geophys. Res.*, *109*, D22101, doi:10.1029/2004JD004878.

Grant, W., et al. (1996), Use of volcanic aerosols to study the tropical stratospheric reservoir, *J. Geophys. Res.*, *101*, 3973–3988.

Hasebe, F. (1994), Quasi-biennial oscillations of ozone and diabatic circulation in the equatorial stratosphere, *J. Atmos. Sci.*, *51*, 729–754.

Haynes, P. H., et al. (1991), On the downward control of extratropical diabatic circulations by eddy-induced mean zonal forces, , *48*, 651–679.

Hollandsworth, S. M., K. P. Bowman, and R. D. McPeters (1995), Observational study of the quasi-biennial oscillation in ozone, *J. Geophys. Res.*, *100*, 7347–7361.

Logan, et al. (2003), Quasibiennial oscillation in tropical ozone as revealed by ozonesonde and satellite data, *J. Geophys. Res.*, *108*(D8), 4244, doi:10.1029/2002JD002170.

Mandel, J. (1964), *The Statistical Analysis of Experimental Data*, Dover Publications, Mineola, New York, 410 pp.

Mote, P. W., K. H. Rosenlof, M. E. McIntyre, E. S. Carr, J. C. Gille, J. R. Holton, J. S. Kinnersley, H. C. Pumphrey, J. M. Russell, and J. W. Waters (1996), An atmospheric tape recorder: The imprint of tropical tropopause temperatures on stratospheric water vapor, *J. Geophys. Res.*, *101*, 3989–4006.

Mote, P. W., T. J. Dunkerton, M. E. McIntyre, E. A. Ray, P. H. Haynes, and J. M. Russell III (1998), Vertical velocity, vertical diffusion and dilution by midlatitude air in the tropical lower stratosphere, *J. Geophys. Res.*, *103*, 8651–8666.

Plumb, R. A., and R. C. Bell (1982), A model of the quasi-biennial oscillation on an equatorial beta-plane, *Q. J. R. Meteorol. Soc.*, *108*, 335–352.

Randel, W., and F. Wu (1996), Isolation of the ozone QBO in SAGE II data by singular-value decomposition, *J. Atmos. Sci.*, *53*, 2546–2559.

Randel, W., F. Wu, J. M. Russell III, and J. W. Waters (1998), Seasonal cycles and QBO variations in stratospheric CH_4 and H_2O observed in UARS HALOE data, *J. Atmos. Sci.*, *55*, 163–185.

Randel, W. J., F. Wu, A. Gettelman, J. M. Russell, J. M. Zawodny, and S. J. Oltmans (2001), Seasonal variation of water vapor in the lower stratosphere observed in Halogen Occultation Experiment data, *J. Geophys. Res.*, *106*, 14,313–14,326.

Randel, W. J., et al. (2004), The SPARC intercomparison of middle-atmosphere climatologies, *J. Clim.*, *17*, 986–1003.

Randel, W. J., F. Wu, H. Vömel, G. E. Nedoluha, and P. Forster (2006), Decreases in stratospheric water vapor after 2001, Links to changes in the tropical tropopause and the Brewer-Dobson circulation, *J. Geophys. Res.*, *111*, D12312, doi:10.1029/2005JD006744.

Randel, W., M. Park, F. Wu, and N. Livesey (2007), A large annual cycle in ozone above the tropical tropopause linked to the Brewer-Dobson circulation, *J. Atmos. Sci.*, *64*, 4479–4488.

Rosenfield, J. E., P. A. Newman, and M. R. Schoeberl (1994), Computations of diabatic descent in the stratospheric polar vortex, *J. Geophys. Res.*, *99*, 16,677–16,689.

Rosenlof, K. H., A. F. Tuck, K. K. Kelly, J. M. Russell, and M. P. McCormick (1997), Hemispheric asymmetries in water vapor and inferences about transport in the lower stratosphere, *J. Geophys. Res.*, *102*, 13,213–13,234.

Russell, J. M., III, A. F. Tuck, L. L. Gordley, J. H. Park, S. R. Drayson, J. E. Harries, R. J. Cicerone, and P. J. Crutzen (1993), The HALOGEN Occultation Experiment, *J. Geophys. Res.*, *98*, 10,777–10,797.

Santee, M. L., et al. (2005), Polar processing and development of the 2004 Antarctic ozone hole: First results from MLS on Aura, *Geophys. Res. Lett.*, *32*, L12817, doi:10.1029/2005GL022582.

Schoeberl, M. R., A. E. Roche, J. M. Russell III, D. Ortland, P. B. Hays, and J. W. Waters (1997), An estimation of the dynamical isolation of the tropical lower stratosphere using trace gas observations of the quasi-biennial oscillation, *Geophys. Res. Lett.*, *24*, 53–56.

Schoeberl, M. R., B. N. Duncan, A. R. Douglass, J. Waters, N. Livesey, W. Read, and M. Filipiak (2006), The carbon monoxide tape recorder, *Geophys. Res. Lett.*, *33*, L12811, doi:10.1029/2006GL026178.

Swinbank, R., and A. O'Niell (1994), A stratosphere-troposphere data assimilation system, *Mon. Weather Rev.*, *122*, 686–702.

Trepte, C. R., and M. Hitchman (1992), Tropical stratospheric circulation deduced from satellite aerosol data, *Nature*, *335*, 626–628.

Waugh, T. M., and D. W. Hall (2002), Age of stratospheric air: Theory, observations and models, *Rev. Geophys.*, *40*(4), 1010, doi:10.1029/2000RG000101.

Waters, J., et al. (2006), The Earth Observing System Microwave Limb Sounder 16 (EOS MLS) on the Aura satellite, *IEEE Trans. Geosci. Remote Sens.*, *44*, 1075–1092.

Zawodny, J. M., and M. P. McCormick (1991), Stratospheric Aerosol and Gas Experiment II: Measurements of the quasi-biennial oscillation in ozone and nitrogen dioxide, *J. Geophys. Res.*, *96*, 9371–9377.

A. R. Douglass, P. A. Newman, and M. R. Schoeberl, NASA Goddard Space Flight Center, Code 916, Bldg. 33, Rm. E311A, Greenbelt, MD 20771-0001, USA. (schom@zephyr.gsfc.nasa.gov)

M. J. Filipiak and H. C. Pumphrey, School of GeoSciences, The University of Edinburgh, Edinburgh, UK.

L. Froidevaux, A. Lambert, N. Livesey, W. Read, and J. Waters, NASA Jet Propulsion Laboratory, Pasadena, CA, USA.

L. R. Lait and D. Lary, University of Maryland Baltimore County, Baltimore, MD, USA.